

Measurement of the Absolute Branching Fractions for $D_s^- \rightarrow \ell^- \bar{\nu}_\ell$ and Extraction of the Decay Constant f_{D_s}

P. del Amo Sanchez,¹ J. P. Lees,¹ V. Poireau,¹ E. Prencipe,¹ V. Tisserand,¹ J. Garra Tico,² E. Grauges,² M. Martinelli^{ab,3} A. Palano^{ab,3} M. Pappagallo^{ab,3} G. Eigen,⁴ B. Stugu,⁴ L. Sun,⁴ M. Battaglia,⁵ D. N. Brown,⁵ B. Hooberman,⁵ L. T. Kerth,⁵ Yu. G. Kolomensky,⁵ G. Lynch,⁵ I. L. Osipenko,⁵ T. Tanabe,⁵ C. M. Hawkes,⁶ A. T. Watson,⁶ H. Koch,⁷ T. Schroeder,⁷ D. J. Asgeirsson,⁸ C. Hearty,⁸ T. S. Mattison,⁸ J. A. McKenna,⁸ A. Khan,⁹ A. Randle-Conde,⁹ V. E. Blinov,¹⁰ A. R. Buzykaev,¹⁰ V. P. Druzhinin,¹⁰ V. B. Golubev,¹⁰ A. P. Onuchin,¹⁰ S. I. Serednyakov,¹⁰ Yu. I. Skovpen,¹⁰ E. P. Solodov,¹⁰ K. Yu. Todyshev,¹⁰ A. N. Yushkov,¹⁰ M. Bondioli,¹¹ S. Curry,¹¹ D. Kirkby,¹¹ A. J. Lankford,¹¹ M. Mandelkern,¹¹ E. C. Martin,¹¹ D. P. Stoker,¹¹ H. Atmacan,¹² J. W. Gary,¹² F. Liu,¹² O. Long,¹² G. M. Vitug,¹² C. Campagnari,¹³ T. M. Hong,¹³ D. Kovalskyi,¹³ J. D. Richman,¹³ C. West,¹³ A. M. Eisner,¹⁴ C. A. Heusch,¹⁴ J. Kroseberg,¹⁴ W. S. Lockman,¹⁴ A. J. Martinez,¹⁴ T. Schalk,¹⁴ B. A. Schumm,¹⁴ A. Seiden,¹⁴ L. O. Winstrom,¹⁴ C. H. Cheng,¹⁵ D. A. Doll,¹⁵ B. Echenard,¹⁵ D. G. Hitlin,¹⁵ P. Ongmongkolkul,¹⁵ F. C. Porter,¹⁵ A. Y. Rakitin,¹⁵ R. Andreassen,¹⁶ M. S. Dubrovin,¹⁶ G. Mancinelli,¹⁶ B. T. Meadows,¹⁶ M. D. Sokoloff,¹⁶ P. C. Bloom,¹⁷ W. T. Ford,¹⁷ A. Gaz,¹⁷ M. Nagel,¹⁷ U. Nauenberg,¹⁷ J. G. Smith,¹⁷ S. R. Wagner,¹⁷ R. Ayad,^{18,*} W. H. Toki,¹⁸ H. Jasper,¹⁹ T. M. Karbach,¹⁹ J. Merkel,¹⁹ A. Petzold,¹⁹ B. Spaan,¹⁹ K. Wacker,¹⁹ M. J. Kobel,²⁰ K. R. Schubert,²⁰ R. Schwierz,²⁰ D. Bernard,²¹ M. Verderi,²¹ P. J. Clark,²² S. Playfer,²² J. E. Watson,²² M. Andreotti^{ab,23} D. Bettoni^{a,23} C. Bozzi^{a,23} R. Calabrese^{ab,23} A. Cecchi^{ab,23} G. Cibinetto^{ab,23} E. Fioravanti^{ab,23} P. Franchini^{ab,23} E. Luppi^{ab,23} M. Munerato^{ab,23} M. Negrini^{ab,23} A. Petrella^{ab,23} L. Piemontese^{a,23} R. Baldini-Ferrolli,²⁴ A. Calcaterra,²⁴ R. de Sangro,²⁴ G. Finocchiaro,²⁴ M. Nicolaci,²⁴ S. Pacetti,²⁴ P. Patteri,²⁴ I. M. Peruzzi,^{24,†} M. Piccolo,²⁴ M. Rama,²⁴ A. Zallo,²⁴ R. Contri^{ab,25} E. Guido^{ab,25} M. Lo Vetere^{ab,25} M. R. Monge^{ab,25} S. Passaggio^{a,25} C. Patrignani^{ab,25} E. Robutti^{a,25} S. Tosi^{ab,25} B. Bhuyan,²⁶ V. Prasad,²⁶ C. L. Lee,²⁷ M. Morii,²⁷ A. Adametz,²⁸ J. Marks,²⁸ U. Uwer,²⁸ F. U. Bernlochner,²⁹ M. Ebert,²⁹ H. M. Lacker,²⁹ T. Lueck,²⁹ A. Volk,²⁹ P. D. Dauncey,³⁰ M. Tibbetts,³⁰ P. K. Behera,³¹ U. Mallik,³¹ C. Chen,³² J. Cochran,³² H. B. Crawley,³² L. Dong,³² W. T. Meyer,³² S. Prell,³² E. I. Rosenberg,³² A. E. Rubin,³² A. V. Gritsan,³³ Z. J. Guo,³³ N. Arnaud,³⁴ M. Davier,³⁴ D. Derkach,³⁴ J. Firmino da Costa,³⁴ G. Grosdidier,³⁴ F. Le Diberder,³⁴ A. M. Lutz,³⁴ B. Malaescu,³⁴ A. Perez,³⁴ P. Roudeau,³⁴ M. H. Schune,³⁴ J. Serrano,³⁴ V. Sordini,^{34,‡} A. Stocchi,³⁴ L. Wang,³⁴ G. Wormser,³⁴ D. J. Lange,³⁵ D. M. Wright,³⁵ I. Bingham,³⁶ C. A. Chavez,³⁶ J. P. Coleman,³⁶ J. R. Fry,³⁶ E. Gabathuler,³⁶ R. Gamet,³⁶ D. E. Hutchcroft,³⁶ D. J. Payne,³⁶ C. Touramanis,³⁶ A. J. Bevan,³⁷ F. Di Lodovico,³⁷ R. Sacco,³⁷ M. Sigamani,³⁷ G. Cowan,³⁸ S. Paramesvaran,³⁸ A. C. Wren,³⁸ D. N. Brown,³⁹ C. L. Davis,³⁹ A. G. Denig,⁴⁰ M. Fritsch,⁴⁰ W. Gradl,⁴⁰ A. Hafner,⁴⁰ K. E. Alwyn,⁴¹ D. Bailey,⁴¹ R. J. Barlow,⁴¹ G. Jackson,⁴¹ G. D. Lafferty,⁴¹ J. Anderson,⁴² R. Cenci,⁴² A. Jawahery,⁴² D. A. Roberts,⁴² G. Simi,⁴² J. M. Tuggle,⁴² C. Dallapiccola,⁴³ E. Salvati,⁴³ R. Cowan,⁴⁴ D. Dujmic,⁴⁴ G. Sciolla,⁴⁴ M. Zhao,⁴⁴ D. Lindemann,⁴⁵ P. M. Patel,⁴⁵ S. H. Robertson,⁴⁵ M. Schram,⁴⁵ P. Biassoni^{ab,46} A. Lazzaro^{ab,46} V. Lombardo^{a,46} F. Palombo^{ab,46} S. Stracka^{ab,46} L. Cremaldi,⁴⁷ R. Godang,^{47,§} R. Kroeger,⁴⁷ P. Sonnek,⁴⁷ D. J. Summers,⁴⁷ X. Nguyen,⁴⁸ M. Simard,⁴⁸ P. Taras,⁴⁸ G. De Nardo^{ab,49} D. Monorchio^{ab,49} G. Onorato^{ab,49} C. Sciacca^{ab,49} G. Raven,⁵⁰ H. L. Snoek,⁵⁰ C. P. Jessop,⁵¹ K. J. Knoepfel,⁵¹ J. M. LoSecco,⁵¹ W. F. Wang,⁵¹ L. A. Corwin,⁵² K. Honscheid,⁵² R. Kass,⁵² J. P. Morris,⁵² N. L. Blount,⁵³ J. Brau,⁵³ R. Frey,⁵³ O. Igonkina,⁵³ J. A. Kolb,⁵³ R. Rahmat,⁵³ N. B. Sinev,⁵³ D. Strom,⁵³ J. Strube,⁵³ E. Torrence,⁵³ G. Castelli^{ab,54} E. Feltresi^{ab,54} N. Gagliardi^{ab,54} M. Margoni^{ab,54} M. Morandin^{a,54} M. Posocco^{a,54} M. Rotondo^{a,54} F. Simonetto^{ab,54} R. Stroili^{ab,54} E. Ben-Haim,⁵⁵ G. R. Bonneaud,⁵⁵ H. Briand,⁵⁵ G. Calderini,⁵⁵ J. Chauveau,⁵⁵ O. Hamon,⁵⁵ Ph. Leruste,⁵⁵ G. Marchiori,⁵⁵ J. Ocariz,⁵⁵ J. Prendki,⁵⁵ S. Sitt,⁵⁵ M. Biasini^{ab,56} E. Manoni^{ab,56} A. Rossi^{ab,56} C. Angelini^{ab,57} G. Batignani^{ab,57} S. Bettarini^{ab,57} M. Carpinelli^{ab,57,¶} G. Casarosa^{ab,57} A. Cervelli^{ab,57} F. Forti^{ab,57} M. A. Giorgi^{ab,57} A. Lusiani^{ac,57} N. Neri^{ab,57} E. Paoloni^{ab,57} G. Rizzo^{ab,57} J. J. Walsh^{a,57} D. Lopes Pegna,⁵⁸ C. Lu,⁵⁸ J. Olsen,⁵⁸ A. J. S. Smith,⁵⁸ A. V. Telnov,⁵⁸ F. Anulli^{a,59} E. Baracchini^{ab,59} G. Cavoto^{a,59} R. Faccini^{ab,59} F. Ferrarotto^{a,59} F. Ferroni^{ab,59} M. Gaspero^{ab,59} L. Li Gioia^{a,59} M. A. Mazzoni^{a,59} G. Piredda^{a,59} F. Renga^{ab,59} T. Hartmann,⁶⁰ T. Leddig,⁶⁰ H. Schröder,⁶⁰ R. Waldi,⁶⁰ T. Adye,⁶¹ B. Franek,⁶¹ E. O. Olaiya,⁶¹ F. F. Wilson,⁶¹ S. Emery,⁶² G. Hamel de Monchenault,⁶² G. Vasseur,⁶² Ch. Yèche,⁶²

M. Zito,⁶² M. T. Allen,⁶³ D. Aston,⁶³ D. J. Bard,⁶³ R. Bartoldus,⁶³ J. F. Benitez,⁶³ C. Cartaro,⁶³ M. R. Convery,⁶³ J. Dorfan,⁶³ G. P. Dubois-Felsmann,⁶³ W. Dunwoodie,⁶³ R. C. Field,⁶³ M. Franco Sevilla,⁶³ B. G. Fulsom,⁶³ A. M. Gabareen,⁶³ M. T. Graham,⁶³ P. Grenier,⁶³ C. Hast,⁶³ W. R. Innes,⁶³ M. H. Kelsey,⁶³ H. Kim,⁶³ P. Kim,⁶³ M. L. Kocian,⁶³ D. W. G. S. Leith,⁶³ S. Li,⁶³ B. Lindquist,⁶³ S. Luitz,⁶³ V. Luth,⁶³ H. L. Lynch,⁶³ D. B. MacFarlane,⁶³ H. Marsiske,⁶³ D. R. Muller,⁶³ H. Neal,⁶³ S. Nelson,⁶³ C. P. O'Grady,⁶³ I. Ofte,⁶³ M. Perl,⁶³ T. Pulliam,⁶³ B. N. Ratcliff,⁶³ A. Roodman,⁶³ A. A. Salnikov,⁶³ V. Santoro,⁶³ R. H. Schindler,⁶³ J. Schwiening,⁶³ A. Snyder,⁶³ D. Su,⁶³ M. K. Sullivan,⁶³ S. Sun,⁶³ K. Suzuki,⁶³ J. M. Thompson,⁶³ J. Va'vra,⁶³ A. P. Wagner,⁶³ M. Weaver,⁶³ C. A. West,⁶³ W. J. Wisniewski,⁶³ M. Wittgen,⁶³ D. H. Wright,⁶³ H. W. Wulsin,⁶³ A. K. Yarritu,⁶³ C. C. Young,⁶³ V. Ziegler,⁶³ X. R. Chen,⁶⁴ W. Park,⁶⁴ M. V. Purohit,⁶⁴ R. M. White,⁶⁴ J. R. Wilson,⁶⁴ S. J. Sekula,⁶⁵ M. Bellis,⁶⁶ P. R. Burchat,⁶⁶ A. J. Edwards,⁶⁶ T. S. Miyashita,⁶⁶ S. Ahmed,⁶⁷ M. S. Alam,⁶⁷ J. A. Ernst,⁶⁷ B. Pan,⁶⁷ M. A. Saeed,⁶⁷ S. B. Zain,⁶⁷ N. Guttman,⁶⁸ A. Soffer,⁶⁸ P. Lund,⁶⁹ S. M. Spanier,⁶⁹ R. Eckmann,⁷⁰ J. L. Ritchie,⁷⁰ A. M. Ruland,⁷⁰ C. J. Schilling,⁷⁰ R. F. Schwitters,⁷⁰ B. C. Wray,⁷⁰ J. M. Izen,⁷¹ X. C. Lou,⁷¹ F. Bianchi^{ab,72} D. Gamba^{ab,72} M. Pelliccioni^{ab,72} M. Bomben^{ab,73} L. Lanceri^{ab,73} L. Vitale^{ab,73} N. Lopez-March,⁷⁴ F. Martinez-Vidal,⁷⁴ D. A. Milanes,⁷⁴ A. Oyanguren,⁷⁴ J. Albert,⁷⁵ Sw. Banerjee,⁷⁵ H. H. F. Choi,⁷⁵ K. Hamano,⁷⁵ G. J. King,⁷⁵ R. Kowalewski,⁷⁵ M. J. Lewczuk,⁷⁵ I. M. Nugent,⁷⁵ J. M. Roney,⁷⁵ R. J. Sobie,⁷⁵ T. J. Gershon,⁷⁶ P. F. Harrison,⁷⁶ T. E. Latham,⁷⁶ E. M. T. Puccio,⁷⁶ H. R. Band,⁷⁷ S. Dasu,⁷⁷ K. T. Flood,⁷⁷ Y. Pan,⁷⁷ R. Prepost,⁷⁷ C. O. Vuosalo,⁷⁷ and S. L. Wu⁷⁷

(The BABAR Collaboration)

¹Laboratoire d'Annecy-le-Vieux de Physique des Particules (LAPP),
Université de Savoie, CNRS/IN2P3, F-74941 Annecy-Le-Vieux, France

²Universitat de Barcelona, Facultat de Física, Departament ECM, E-08028 Barcelona, Spain

³INFN Sezione di Bari^a; Dipartimento di Fisica, Università di Bari^b, I-70126 Bari, Italy

⁴University of Bergen, Institute of Physics, N-5007 Bergen, Norway

⁵Lawrence Berkeley National Laboratory and University of California, Berkeley, California 94720, USA

⁶University of Birmingham, Birmingham, B15 2TT, United Kingdom

⁷Ruhr Universität Bochum, Institut für Experimentalphysik 1, D-44780 Bochum, Germany

⁸University of British Columbia, Vancouver, British Columbia, Canada V6T 1Z1

⁹Brunel University, Uxbridge, Middlesex UB8 3PH, United Kingdom

¹⁰Budker Institute of Nuclear Physics, Novosibirsk 630090, Russia

¹¹University of California at Irvine, Irvine, California 92697, USA

¹²University of California at Riverside, Riverside, California 92521, USA

¹³University of California at Santa Barbara, Santa Barbara, California 93106, USA

¹⁴University of California at Santa Cruz, Institute for Particle Physics, Santa Cruz, California 95064, USA

¹⁵California Institute of Technology, Pasadena, California 91125, USA

¹⁶University of Cincinnati, Cincinnati, Ohio 45221, USA

¹⁷University of Colorado, Boulder, Colorado 80309, USA

¹⁸Colorado State University, Fort Collins, Colorado 80523, USA

¹⁹Technische Universität Dortmund, Fakultät Physik, D-44221 Dortmund, Germany

²⁰Technische Universität Dresden, Institut für Kern- und Teilchenphysik, D-01062 Dresden, Germany

²¹Laboratoire Leprince-Ringuet, CNRS/IN2P3, Ecole Polytechnique, F-91128 Palaiseau, France

²²University of Edinburgh, Edinburgh EH9 3JZ, United Kingdom

²³INFN Sezione di Ferrara^a; Dipartimento di Fisica, Università di Ferrara^b, I-44100 Ferrara, Italy

²⁴INFN Laboratori Nazionali di Frascati, I-00044 Frascati, Italy

²⁵INFN Sezione di Genova^a; Dipartimento di Fisica, Università di Genova^b, I-16146 Genova, Italy

²⁶Indian Institute of Technology Guwahati, Guwahati, Assam, 781 039, India

²⁷Harvard University, Cambridge, Massachusetts 02138, USA

²⁸Universität Heidelberg, Physikalisches Institut, Philosophenweg 12, D-69120 Heidelberg, Germany

²⁹Humboldt-Universität zu Berlin, Institut für Physik, Newtonstr. 15, D-12489 Berlin, Germany

³⁰Imperial College London, London, SW7 2AZ, United Kingdom

³¹University of Iowa, Iowa City, Iowa 52242, USA

³²Iowa State University, Ames, Iowa 50011-3160, USA

³³Johns Hopkins University, Baltimore, Maryland 21218, USA

³⁴Laboratoire de l'Accélérateur Linéaire, IN2P3/CNRS et Université Paris-Sud 11,
Centre Scientifique d'Orsay, B. P. 34, F-91898 Orsay Cedex, France

³⁵Lawrence Livermore National Laboratory, Livermore, California 94550, USA

³⁶University of Liverpool, Liverpool L69 7ZE, United Kingdom

³⁷Queen Mary, University of London, London, E1 4NS, United Kingdom

³⁸University of London, Royal Holloway and Bedford New College, Egham, Surrey TW20 0EX, United Kingdom

³⁹University of Louisville, Louisville, Kentucky 40292, USA

⁴⁰Johannes Gutenberg-Universität Mainz, Institut für Kernphysik, D-55099 Mainz, Germany

- ⁴¹University of Manchester, Manchester M13 9PL, United Kingdom
⁴²University of Maryland, College Park, Maryland 20742, USA
⁴³University of Massachusetts, Amherst, Massachusetts 01003, USA
⁴⁴Massachusetts Institute of Technology, Laboratory for Nuclear Science, Cambridge, Massachusetts 02139, USA
⁴⁵McGill University, Montréal, Québec, Canada H3A 2T8
⁴⁶INFN Sezione di Milano^a; Dipartimento di Fisica, Università di Milano^b, I-20133 Milano, Italy
⁴⁷University of Mississippi, University, Mississippi 38677, USA
⁴⁸Université de Montréal, Physique des Particules, Montréal, Québec, Canada H3C 3J7
⁴⁹INFN Sezione di Napoli^a; Dipartimento di Scienze Fisiche, Università di Napoli Federico II^b, I-80126 Napoli, Italy
⁵⁰NIKHEF, National Institute for Nuclear Physics and High Energy Physics, NL-1009 DB Amsterdam, The Netherlands
⁵¹University of Notre Dame, Notre Dame, Indiana 46556, USA
⁵²Ohio State University, Columbus, Ohio 43210, USA
⁵³University of Oregon, Eugene, Oregon 97403, USA
⁵⁴INFN Sezione di Padova^a; Dipartimento di Fisica, Università di Padova^b, I-35131 Padova, Italy
⁵⁵Laboratoire de Physique Nucléaire et de Hautes Energies, IN2P3/CNRS, Université Pierre et Marie Curie-Paris6, Université Denis Diderot-Paris7, F-75252 Paris, France
⁵⁶INFN Sezione di Perugia^a; Dipartimento di Fisica, Università di Perugia^b, I-06100 Perugia, Italy
⁵⁷INFN Sezione di Pisa^a; Dipartimento di Fisica, Università di Pisa^b; Scuola Normale Superiore di Pisa^c, I-56127 Pisa, Italy
⁵⁸Princeton University, Princeton, New Jersey 08544, USA
⁵⁹INFN Sezione di Roma^a; Dipartimento di Fisica, Università di Roma La Sapienza^b, I-00185 Roma, Italy
⁶⁰Universität Rostock, D-18051 Rostock, Germany
⁶¹Rutherford Appleton Laboratory, Chilton, Didcot, Oxon, OX11 0QX, United Kingdom
⁶²CEA, Irfu, SPP, Centre de Saclay, F-91191 Gif-sur-Yvette, France
⁶³SLAC National Accelerator Laboratory, Stanford, California 94309 USA
⁶⁴University of South Carolina, Columbia, South Carolina 29208, USA
⁶⁵Southern Methodist University, Dallas, Texas 75275, USA
⁶⁶Stanford University, Stanford, California 94305-4060, USA
⁶⁷State University of New York, Albany, New York 12222, USA
⁶⁸Tel Aviv University, School of Physics and Astronomy, Tel Aviv, 69978, Israel
⁶⁹University of Tennessee, Knoxville, Tennessee 37996, USA
⁷⁰University of Texas at Austin, Austin, Texas 78712, USA
⁷¹University of Texas at Dallas, Richardson, Texas 75083, USA
⁷²INFN Sezione di Torino^a; Dipartimento di Fisica Sperimentale, Università di Torino^b, I-10125 Torino, Italy
⁷³INFN Sezione di Trieste^a; Dipartimento di Fisica, Università di Trieste^b, I-34127 Trieste, Italy
⁷⁴IFIC, Universitat de Valencia-CSIC, E-46071 Valencia, Spain
⁷⁵University of Victoria, Victoria, British Columbia, Canada V8W 3P6
⁷⁶Department of Physics, University of Warwick, Coventry CV4 7AL, United Kingdom
⁷⁷University of Wisconsin, Madison, Wisconsin 53706, USA

(Dated: November 7, 2018)

The absolute branching fractions for the decays $D_s^- \rightarrow \ell^- \bar{\nu}_\ell$ ($\ell = e, \mu, \text{ or } \tau$) are measured using a data sample corresponding to an integrated luminosity of 521 fb^{-1} collected at center of mass energies near 10.58 GeV with the BABAR detector at the PEP-II e^+e^- collider at SLAC. The number of D_s^- mesons is determined by reconstructing the recoiling system $DKX\gamma$ in events of the type $e^+e^- \rightarrow DKXD_s^{*-}$, where $D_s^{*-} \rightarrow D_s^- \gamma$ and X represents additional pions from fragmentation. The $D_s^- \rightarrow \ell^- \bar{\nu}_\ell$ events are detected by full or partial reconstruction of the recoiling system $DKX\gamma\ell$. The branching fraction measurements are combined to determine the D_s^- decay constant $f_{D_s} = (258.6 \pm 6.4 \pm 7.5) \text{ MeV}$, where the first uncertainty is statistical and the second is systematic.

PACS numbers: 13.20.Fc, 12.38.Gc

The D_s^- meson can decay purely leptonically via annihilation of the \bar{c} and s quarks into a W^- boson [1]. In the Standard Model (SM), the leptonic partial width $\Gamma(D_s^- \rightarrow \ell^- \bar{\nu}_\ell)$ is given by

$$\Gamma = \frac{G_F^2 M_{D_s}^3}{8\pi} \left(\frac{m_\ell}{M_{D_s}} \right)^2 \left(1 - \frac{m_\ell^2}{M_{D_s}^2} \right)^2 |V_{cs}|^2 f_{D_s}^2, \quad (1)$$

*Now at Temple University, Philadelphia, PA 19122, USA

†Also with Università di Perugia, Perugia, Italy

‡Also with Università di Roma La Sapienza, I-00185 Roma, Italy

§Now at University of South Alabama, Mobile, AL 36688, USA

¶Also with Università di Sassari, Sassari, Italy

where M_{D_s} and m_ℓ are the D_s^- and lepton masses, respectively, G_F is the Fermi coupling constant, and V_{cs} is an element of the Cabibbo-Kobayashi-Maskawa quark mixing matrix. These decays provide a clean probe of the pseudoscalar meson decay constant f_{D_s} .

Within the SM, f_{D_s} has been predicted using several methods [2]; the most precise value by Follana *et al.* uses unquenched LQCD calculations and gives $f_{D_s}=(241 \pm 3)$ MeV. Currently, the experimental values are significantly larger than this theoretical prediction. The Heavy Flavor Averaging Group combines the CLEO-c, Belle and BABAR measurements and reports $f_{D_s}=(254.6 \pm 5.9)$ MeV [3]. Models of new physics (NP), including a two-Higgs doublet [4] and leptoquarks [5], may explain this difference. In addition, f_{D_s} measurements provide a cross-check of QCD calculations which predict the impact of NP on B and B_s meson decay rates and mixing. High precision determinations of f_{D_s} , both from experiment and theory, are necessary in order to discover or constrain effects of NP.

We present absolute measurements of the branching fractions of leptonic D_s^- decays with a method similar to the one used by the Belle Collaboration [6, 7]. An inclusive sample of D_s^- 's is obtained by reconstructing the rest of the event in reactions of the kind $e^+e^- \rightarrow c\bar{c} \rightarrow DKXD_s^{*-}$, where $D_s^{*-} \rightarrow D_s^- \gamma$. Here, D represents a charmed hadron (D^0 , D^+ , D^* , or A_c^+), K represents the K_s^0 or K^+ required to balance strangeness in the event, and X represents additional pions produced in the $c\bar{c}$ fragmentation process. When the charmed hadron is a A_c^+ an additional anti-proton is required to assure baryon number conservation. No requirements are placed on the decay products of the D_s^- so that the selected events correspond to an inclusive sample. The 4-momentum of each D_s^- candidate, p_r , is measured as the difference between the momenta of the colliding beam particles and the fully reconstructed $DKX\gamma$ system: $p_r = p_{e^+} + p_{e^-} - p_D - p_K - p_X - p_\gamma$. The inclusive D_s^- yield is obtained from a binned fit to the distribution in the recoil mass $m_r(DKX\gamma) \equiv \sqrt{p_r^2}$. Within this inclusive sample, we determine the fraction of events corresponding to $D_s^- \rightarrow \mu^- \bar{\nu}_\mu$, $D_s^- \rightarrow e^- \bar{\nu}_e$, and $D_s^- \rightarrow \tau^- \bar{\nu}_\tau$ decays. In the SM, ratios of the branching fractions for these decays are $e^- \bar{\nu}_e : \mu^- \bar{\nu}_\mu : \tau^- \bar{\nu}_\tau = 2 \times 10^{-5} : 1 : 10$, due to helicity and phase-space suppression.

The analysis is based on a data sample of 521 fb^{-1} , which corresponds to about 677 million $e^+e^- \rightarrow c\bar{c}$ events, recorded near $\sqrt{s} = 10.58$ GeV by the BABAR detector at the SLAC PEP-II asymmetric-energy collider. The detector is described in detail in Refs. [8, 9]. Charged-particle momenta are measured with a 5 layer, double-sided silicon vertex tracker (SVT) and a 40 layer drift chamber (DCH) inside a 1.5 T superconducting solenoidal magnet. A calorimeter consisting of 6580 CsI(Tl) crystals (EMC) is used to measure electromagnetic energy. Measurements from a ring-imaging Cherenkov radiation detector, and of specific ionization (dE/dx) in the SVT and DCH, provide particle identi-

fication (PID) of charged hadrons. Muons are mainly identified by the instrumented magnetic flux return, and electrons are identified using EMC and dE/dx information. The analysis uses Monte Carlo (MC) events generated with EvtGen and JETSET [10, 11] and passed through a detailed GEANT4 [12] simulation of the detector response. Final state radiation from charged particles is modeled by PHOTOS [13]. Samples of MC events for e^+e^- annihilation to $q\bar{q}$ ($q = u, d, s, c, b$) (generic MC) are used to develop methods to separate signal events from backgrounds. In addition, we use dedicated samples for D_s^- production and leptonic decays (signal MC) to determine reconstruction efficiencies and the distributions needed for the extraction of the signal decays.

We reconstruct D candidates using the following 15 modes: $D^0 \rightarrow K^- \pi^+ (\pi^0)$, $K^- \pi^+ \pi^- \pi^+ (\pi^0)$, or $K_s^0 \pi^+ \pi^- (\pi^0)$; $D^+ \rightarrow K^- \pi^+ \pi^+ (\pi^0)$, $K_s^0 \pi^+ (\pi^0)$, or $K_s^0 \pi^+ \pi^- \pi^+$; and $A_c^+ \rightarrow p K^- \pi^+ (\pi^0)$, $p K_s^0$, or $p K_s^0 \pi^- \pi^+$. All π^0 's and K_s^0 's used in this analysis are reconstructed from two photons or two oppositely charged pions, respectively, and are kinematically constrained to their nominal mass values [14]. The K_s^0 in a D candidate must have a flight distance from the e^+e^- interaction point (IP) greater than 10 times its uncertainty. For each D candidate we fit the tracks to a common vertex, and for each mode, we determine the mean and σ of the reconstructed signal mass distribution from a fit to data. We then simultaneously optimize a set of selection criteria to maximize $S/\sqrt{S+B}$, where S refers to the number of D candidates after subtraction of the background B within a mass window defined about the signal peak. Where B is estimated from the sideband regions of the mass distribution. In addition to the size of the mass window, several other properties of the D candidate are used in the optimization: the center-of-mass (CM) momentum of the D , PID requirements on the tracks, the probability of the D vertex fit, and the minimum lab energy of π^0 photons. The CM momentum must be at least 2.35 GeV/c in order to remove B meson backgrounds. After the optimization the relative contributions to the total signal sample are 74.0% D^0 , 22.6% D^+ , and 3.4% A_c^+ . Multiple candidates per event are accepted.

To identify D mesons originating from D^* decays we reconstruct the following decays: $D^{*+} \rightarrow D^0 \pi^+$, $D^{*0} \rightarrow D^0 \pi^0$, $D^{*+} \rightarrow D^+ \pi^0$, and $D^{*0} \rightarrow D^0 \gamma$. The photon energy in the laboratory frame is required to exceed 30 MeV for $\pi^0 \rightarrow \gamma\gamma$ and 250 MeV for $D^{*0} \rightarrow D^0 \gamma$ decays. The $\gamma\gamma$ invariant mass must be within 3 sigma of the π^0 peak. For all D^* decays, the mass difference $m(D^*) - m(D)$ is required to be within 2.5 sigma of the peak value.

A K candidate is selected from tracks not overlapping with the D candidate. PID requirements are applied to each K^+ candidate, and a K_s^0 candidate must have a flight distance greater than 5 times its uncertainty.

An X candidate is reconstructed from the remaining π^\pm 's and π^0 s not overlapping with the DK candidate. In the laboratory frame, a π^\pm must have a momentum greater than 100 MeV/c and each photon from a π^0 decay

must have energy greater than 100 MeV. We reconstruct X modes without π^0 's with up to three charged pions, and modes with one π^0 with up to two charged pions. The total charge of the X candidate is not checked at this stage.

Finally, we select a γ candidate for the signal D_s^{*-} decay by requiring a minimum energy of 120 MeV in the laboratory frame, and an angle with respect to the direction of the D candidate momentum in the CM frame greater than 90 degrees. This photon cannot form a π^0 or η candidate when combined with any other photon in the event. In addition, the cluster must pass tight requirements on the shower shape in the EMC and a separation of at least 15 cm from the impact of any charged particle or the position of any other energy cluster in the EMC.

Only $DKX\gamma$ candidates with a total charge of +1 are selected to form a right-sign (RS) sample, from which we extract the D_s^- signal yield. The charm and strange quark content of the DKX must be consistent with recoiling from a D_s^- . The RS sample includes candidates for which consistency cannot be determined due to the presence of a K_s^0 . We define a wrong-sign (WS) sample with the same charge requirement above, but by requiring that the charm and strange quark content of the DKX be consistent with a recoil from a D_s^+ . The WS sample contains a small fraction of signal events due mainly to DKX candidates for which the total charge is misreconstructed. The generic MC shows that the WS sample, after subtraction of the signal contribution, correctly models the backgrounds in the RS sample.

A kinematic fit to each DKX candidate is performed in which the particles are required to originate from a common point inside the IP region, and the D mass is constrained to the nominal value [14]. The 4-momentum of the signal D_s^{*-} is extracted as the missing 4-momentum in the event. We require that the D_s^{*-} candidate mass be within 2.5σ of the signal peak. For MC signal events, the mean is found to be consistent with the nominal value and σ varies between 37 and 64 MeV/ c^2 depending on the number of pions in X.

We perform a similar kinematic fit with the signal γ included and with the mass recoiling against the DKX constrained to the nominal D_s^{*-} mass [14] in order to determine the D_s^- 4-momentum. We require that the D_s^- CM momentum exceed 3.0 GeV/ c , and that its mass be greater than 1.82 GeV/ c^2 . After the final selections, there remain on average 1.7 D_s^- candidates per event, due mainly to multiple photons that can be associated with the D_s^{*-} decay. In order to properly count events in the fits described below, we assign weight $1/n$ to each D_s^- candidate, where n is the number of D_s^- candidates in the event.

We define n_X^R and n_X^T to be the number of reconstructed and true pions in the X system, respectively. The efficiency for reconstructing signal events depends on n_X^T . However, the n_X^T distribution is expected to differ from the MC simulation due to inaccurate fragmentation functions used by JETSET. To correct for these

inaccuracies, we extract the D_s^- signal yields from a fit to the two-dimensional histogram of $m_r(DKX\gamma)$ versus n_X^R . The PDF for the signal distribution is written as a weighted sum of the MC distributions for $j = n_X^T$,

$$S(m, n_X^R) = \sum_{j=0}^6 w_j S_j(m, n_X^R). \quad (2)$$

The weights w_j have to be extracted from this fit. To constrain the shape of the weights distribution, we introduce the parameterization $w_j \propto (j - \alpha)^\beta e^{-\gamma j}$ together with the condition $\sum_j w_j = 1$. This parameterization is motivated by the distribution of weights in the MC. The value $\alpha = -1.32$ is taken from a fit to MC, whereas β and γ are determined from the fit to data.

The RS and WS samples are fitted simultaneously to determine the background. The fit to the WS sample uses a signal component similar to that used in the RS fit, except that due to the small signal component, the weights are fixed to the MC values and the signal yield is determined from signal MC to be 11.8% of the RS signal yield. The shapes remaining after the signal component is removed from the WS sample, $B_i(m)$ ($i = n_X^R$), are used to model the RS backgrounds. A shape correction is applied to B_0 to account for a difference observed in the MC. We add these components with free coefficients (b_i) to construct the total RS background shape: $B(m, n_X^R) = \sum_{i=0}^3 b_i B_i(m) \delta(i - n_X^R)$. Thus in addition to β , γ , and the total signal yield, there are 3 additional free parameters b_i ($i = 0, 1, 2$) in the RS fit.

Figure 1 shows the data and the results of the fit, and Fig. 2 shows the total RS and WS samples. The fit finds a minimum $\chi^2/ndf = 216/182$ and the fitted parameter values are $\beta = 0.27 \pm 0.17$ and $\gamma = 0.28 \pm 0.07$. These are different from the MC values $\beta = 3.38$ and $\gamma = 1.15$ since there are more events at low values of n_X^T than in the MC.

Having constructed the inclusive D_s^- sample, we proceed to the selection of $D_s^- \rightarrow \mu^- \bar{\nu}_\mu$ events within that sample. We use the $m_r(DKX\gamma)$ range between 1.934 and 2.012 GeV/ c^2 , which contains an inclusive D_s^- yield ($N_{D_s^-}$) of $(67.2 \pm 1.5) \times 10^3$. We require that there be exactly one more charged particle in the remainder of the event, and that it be identified as a μ^- . In addition, we require that the extra neutral energy in the event, E_{extra} , be less than 1.0 GeV; E_{extra} is defined as the total energy of EMC clusters with individual energy greater than 30 MeV and not overlapping with the $DKX\gamma$ candidate. Since the only missing particle in the event should be the neutrino we expect the distribution of E_{extra} to peak at zero for signal events. We determine the 4-momentum of the $\bar{\nu}_\mu$ candidate through a kinematic fit similar to that described earlier in the determination of the D_s^- 4-momentum, but with the μ^- included in the recoil system. In this fit we constrain the mass recoiling against the $DKX\gamma$ system to the nominal value for the D_s^- [14]. To extract the signal yield, we perform a binned maximum likelihood fit to the $m_r^2(DKX\gamma\mu)$ distribu-

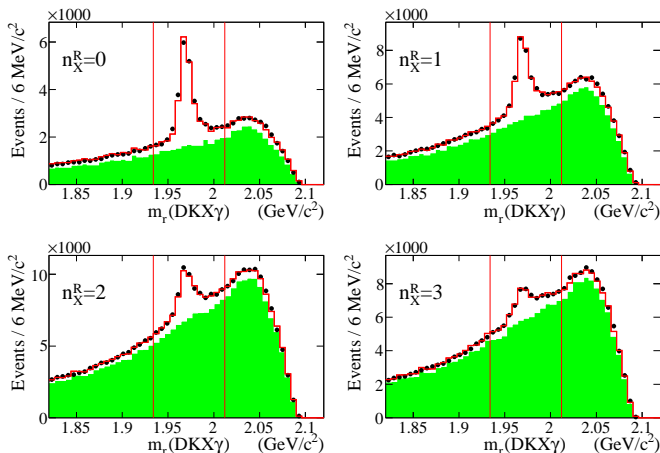


FIG. 1: (color online) $m_r(DKX\gamma)$ distributions for each n_X^R value. The points are the data. The open histogram is from the fit described in the text. The solid histogram is the background component from the fit. The vertical lines define the region used in the $\ell^-\bar{\nu}_\ell$ selections.

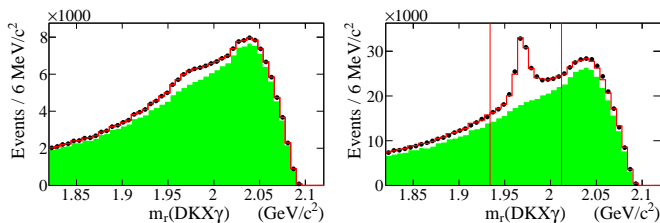


FIG. 2: (color online) $m_r(DKX\gamma)$ distribution for the total WS (left) and RS (right) samples.

tion using a signal PDF determined from reconstructed signal MC events that contain the signal decay chain $D_s^{*-} \rightarrow D_s^- \gamma$ with $D_s^- \rightarrow \mu^- \bar{\nu}_\mu$. The background PDF is determined from the reconstructed generic MC events with signal events removed. The fit is shown in Fig. 3(a), and the number of signal events extracted, $N_{\mu\nu}$, is listed in Table I.

The $D_s^- \rightarrow \mu^- \bar{\nu}_\mu$ branching fraction is obtained from:

$$\mathcal{B}(D_s^- \rightarrow \mu^- \bar{\nu}_\mu) = \frac{N_{\mu\nu}}{N_{D_s} \sum_{j=0}^6 w_j \frac{\varepsilon_{D_s}^j}{\varepsilon_{D_s}^j}} = \frac{N_{\mu\nu}}{N_{D_s} \bar{\varepsilon}_{\mu\nu}}, \quad (3)$$

where the $D_s^- \rightarrow \mu^- \bar{\nu}_\mu$ reconstruction efficiency, $\varepsilon_{\mu\nu}^j$, is determined using the signal MC sample with $j = n_X^T$, and $\varepsilon_{D_s}^j$ is the corresponding inclusive D_s^- reconstruction efficiency. The efficiency ratios $\varepsilon_{\mu\nu}^j / \varepsilon_{D_s}^j$ decrease from 87% to 33% as j increases from 0 to 6. The weighted average, $\bar{\varepsilon}_{\mu\nu}$, and the value determined for $\mathcal{B}(D_s^- \rightarrow \mu^- \bar{\nu}_\mu)$ are listed in Table I. The statistical uncertainty includes contributions from N_{D_s} , $\bar{\varepsilon}_{\mu\nu}$, and $N_{\mu\nu}$ (with correlations taken into account). The systematic uncertainty is determined by varying the parameter values in the inclusive D_s^- fit which were fixed to MC values, by varying

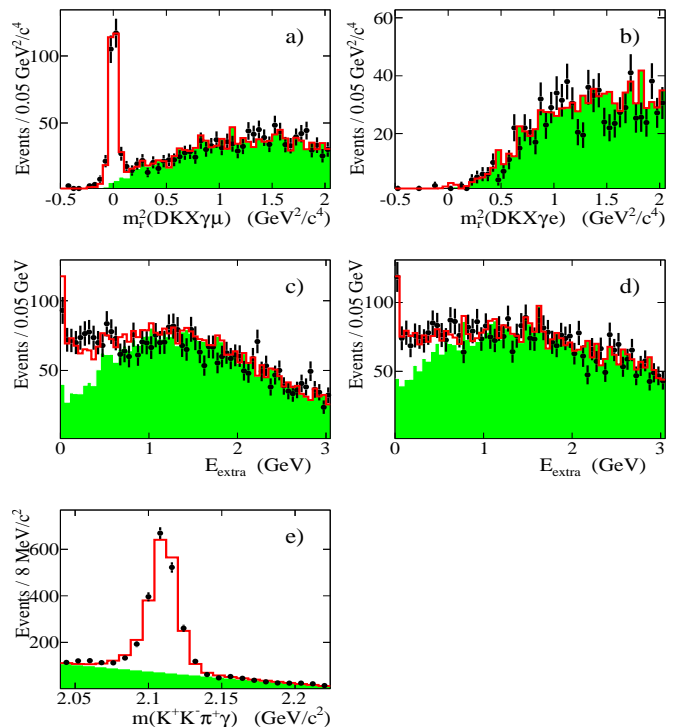


FIG. 3: (color online) Fitted distributions of (a) $m_r^2(DKX\gamma\mu)$, (b) $m_r^2(DKX\gamma e)$, (c) E_{extra} for $D_s^- \rightarrow \tau_{e\nu\nu}\bar{\nu}_\tau$, (d) E_{extra} for $D_s^- \rightarrow \tau_{\mu\nu\nu}\bar{\nu}_\tau$ candidates, and (e) $m(KK\pi\gamma)$. In each figure, the points represent the data with statistical error bars, the open histogram is from the fit described in the text, and the solid histogram is the background component from the fit.

the resolution on the D_s^- signal PDF (for both mass and n_X^R), and by estimating how well the MC models the non-peaking component of the signal PDF observed in Figs. 1 and 2. The non-peaking signal component in the $m_r(DKX\gamma)$ distribution arises from $DKX\gamma$ candidates in events that contain the signal decay $D_s^{*-} \rightarrow D_s^- \gamma$, but for which the photon candidate is mis-identified and is due to other sources such as π^0 or η decays, or tracks or K_L^0 interacting in the calorimeter. Uncertainties are assigned for possible mismodeling of the signal or background $m_r^2(DKX\gamma\mu)$ distributions due to possible differences in the position or resolution of the mass distribution, or mismodelings of different D_s^- decays. Uncertainties in the efficiencies due to tracking and μ^- identification are included. This measurement supersedes our previous result [15].

Using a procedure similar to that for $D_s^- \rightarrow \mu^- \bar{\nu}_\mu$ we search for $D_s^- \rightarrow e^- \bar{\nu}_e$ events. The fit to the $m_r^2(DKX\gamma e)$ distribution, shown in Fig. 3(b), gives a signal yield $N_{e\nu}$ consistent with 0. We obtain an upper limit on $\mathcal{B}(D_s^- \rightarrow e^- \bar{\nu}_e)$ by integrating a likelihood function from 0 to the value of $\mathcal{B}(D_s^- \rightarrow e^- \bar{\nu}_e)$ corresponding to 90% of the integral from 0 to infinity. The likelihood function consists of a Gaussian function written in terms of the variable $\mathcal{B}N_{D_s} \bar{\varepsilon}_{e\nu}$ with mean and sigma

TABLE I: Average efficiency ratios, signal yields, branching fractions, and decay constants for the leptonic D_s^- decays. The first uncertainty is statistical and the second is systematic.

Decay	$\bar{\varepsilon}$	Signal Yield	$\mathcal{B}(D_s^- \rightarrow \ell^- \bar{\nu}_\ell)$	f_{D_s} (MeV)
$D_s^- \rightarrow e^- \bar{\nu}_e$	70.5%	$6.1 \pm 2.2 \pm 5.2$	$< 2.3 \times 10^{-4}$ at 90% C.L.	
$D_s^- \rightarrow \mu^- \bar{\nu}_\mu$	67.7%	275 ± 17	$(6.02 \pm 0.38 \pm 0.34) \times 10^{-3}$	$265.7 \pm 8.4 \pm 7.7$
$D_s^- \rightarrow \tau^- \bar{\nu}_\tau$ ($\tau^- \rightarrow e^- \bar{\nu}_e \nu_\tau$)	61.6%	408 ± 42	$(5.07 \pm 0.52 \pm 0.68) \times 10^{-2}$	$247 \pm 13 \pm 17$
$D_s^- \rightarrow \tau^- \bar{\nu}_\tau$ ($\tau^- \rightarrow \mu^- \bar{\nu}_\mu \nu_\tau$)	59.5%	340 ± 32	$(4.91 \pm 0.47 \pm 0.54) \times 10^{-2}$	$243 \pm 12 \pm 14$

set to $N_{e\nu}$ and its total uncertainty, respectively. To account for the uncertainties on $N_{D_s} \bar{\varepsilon}_{e\nu}$, the main Gaussian is convolved with another Gaussian function centered at the measured value of $N_{D_s} \bar{\varepsilon}_{e\nu}$ with sigma set to the $N_{D_s} \bar{\varepsilon}_{e\nu}$ total uncertainty. The value obtained for the upper limit is listed in Table I.

We find $D_s^- \rightarrow \tau^- \bar{\nu}_\tau$ decays within the sample of inclusively reconstructed D_s^- events by requiring exactly one more track identified as an e^- or μ^- , from the decay $\tau^- \rightarrow e^- \bar{\nu}_e \nu_\tau$ or $\tau^- \rightarrow \mu^- \bar{\nu}_\mu \nu_\tau$. We remove events associated with $D_s^- \rightarrow \mu^- \bar{\nu}_\mu$ decays by requiring $m_\tau^2(DKX\gamma\mu) > 0.5 \text{ GeV}^2/c^4$. Since $D_s^- \rightarrow \tau^- \bar{\nu}_\tau$ events contain more than one neutrino we use E_{extra} to extract the yield of signal events; these are expected to peak towards zero, while the backgrounds extend over a wide range. The signal and background PDFs are determined from reconstructed MC event samples. The fits are shown in Figs. 3(c) and 3(d); the signal yields are listed in Table I. We determine $\mathcal{B}(D_s^- \rightarrow \tau^- \bar{\nu}_\tau)$ from the e^- and μ^- samples using Eq. (3) and accounting for the decay fractions of the τ^- [14]. The values obtained are listed in Table I and are consistent with the previous *BABAR* result [16]. The error-weighted average [17] of the branching fractions is $\mathcal{B}(D_s^- \rightarrow \tau^- \bar{\nu}_\tau) = (5.00 \pm 0.35(stat) \pm 0.49(syst)) \times 10^{-2}$. The weights used in the average are computed from the total error matrix and account for correlations. As a test of lepton flavor universality we determine the ratio $\mathcal{B}(D_s^- \rightarrow \tau^- \bar{\nu}_\tau)/\mathcal{B}(D_s^- \rightarrow \mu^- \bar{\nu}_\mu) = (8.27 \pm 0.77(stat) \pm 0.85(syst))$, which is consistent with the SM value of 9.76.

As a cross-check of this analysis method, we measure the branching fraction for the hadronic decay $D_s^- \rightarrow K^- K^+ \pi^-$. Within the inclusive D_s^- sample, we require exactly three additional charged particle tracks that do not overlap with the $DKX\gamma$ candidate. PID requirements are applied to the kaon candidates. The mass of the $K^- K^+ \pi^-$ system must be between 1.93 and 2.00 GeV/c^2 , and the CM momentum above 3.0 GeV/c . We combine the $K^- K^+ \pi^-$ system with the signal γ and extract the signal yield from the $m(KK\pi\gamma)$ distribution. For this mode we choose the loose selection $m_\tau(DKX\gamma) > 1.82 \text{ GeV}/c^2$, because this variable is correlated with $m(KK\pi\gamma)$; this corresponds to an inclusive D_s^- yield of $N_{D_s} = (108.9 \pm 2.4) \times 10^3$. We model the signal distribution using reconstructed MC events that contain the decay chain $D_s^{*-} \rightarrow D_s^- \gamma$ and $D_s^- \rightarrow K^- K^+ \pi^-$. In the generic MC and a high statistics control data sample (for which the inclusive recon-

struction was not applied) the background was found to be linear in $m(KK\pi\gamma)$. From a fit to the $m(KK\pi\gamma)$ distribution, shown in Fig. 3(e), we determine a signal yield of $N_{KK\pi} = 1866 \pm 40$ events.

We compute the $D_s^- \rightarrow K^- K^+ \pi^-$ branching fraction using Eq. (3). The efficiency for reconstructing signal events is determined from the signal MC in three regions of the $K^- K^+ \pi^-$ Dalitz plot, corresponding to $\phi\pi^-$, $K^- K^{*0}$, and the rest. A variation of $\sim 8\%$ is observed across the Dalitz plot, leading to a correction factor of 1.016 on $\varepsilon_{KK\pi}^j$. The weighted efficiency ratio is found to be $\bar{\varepsilon}_{KK\pi} = 29.5\%$, and we obtain $\mathcal{B}(D_s^- \rightarrow K^- K^+ \pi^-) = (5.78 \pm 0.20(stat) \pm 0.30(syst))\%$. The first uncertainty accounts for the statistical uncertainties associated with the inclusive D_s^- sample and $N_{KK\pi}$. The second accounts for systematic uncertainties in the signal and background models, and the inclusive D_s^- sample, as well as the reconstruction and PID selection of the $K^- K^+ \pi^-$ candidates. This result is consistent with the value $(5.50 \pm 0.23 \pm 0.16)\%$ measured by CLEO-c [18].

Using the leptonic branching fractions measured above, we determine the D_s^- decay constant using Eq. (1) and the known values for m_ℓ , m_{D_s} , $|V_{ud}|$ (we assume $|V_{cs}| = |V_{ud}|$), and the D_s^- lifetime obtained from Ref. [14]. The f_{D_s} values are listed in Table I; the systematic uncertainty includes the uncertainties on these parameters (1.9 MeV). Finally, we obtain the error-weighted average $f_{D_s} = (258.6 \pm 6.4(stat) \pm 7.5(syst))$ MeV.

In conclusion, we use the full dataset collected by the *BABAR* experiment to measure the branching fractions for the leptonic decays of the D_s^- meson. The measured value of f_{D_s} is 1.8 standard deviations larger than the theoretical value [2], consistent with the measurements by Belle and CLEO-c [6, 19]. Further work on this subject is necessary to validate the theoretical calculations or to shed light on possible NP processes.

We are grateful for the excellent luminosity and machine conditions provided by our PEP-II colleagues, and for the substantial dedicated effort from the computing organizations that support *BABAR*. The collaborating institutions wish to thank SLAC for its support and kind hospitality. This work is supported by DOE and NSF (USA), NSERC (Canada), CEA and CNRS-IN2P3 (France), BMBF and DFG (Germany), INFN (Italy), FOM (The Netherlands), NFR (Norway), MES (Russia), MICIIN (Spain), STFC (United Kingdom). Individuals have received support from the Marie Curie EIF (Euro-

pean Union), the A. P. Sloan Foundation (USA) and the Binational Science Foundation (USA-Israel).

-
- [1] Use of charge conjugate reactions is implied in this paper.
- [2] E. Follana *et al.*, Phys. Rev. Lett. **100**, 062002 (2008); A. Ali Khan *et al.*, Phys.Lett.B **652**, 150 (2007); C. Aubin *et al.*, Phys.Rev.Lett. **95**, 122002 (2005); B. Blossier *et al.*, JHEP **0907**, 043 (2009); C. Bernard *et al.*, PoS LATTICE2008, 278 (2008); J. Bordes *et al.*, JHEP **0511**, 014 (2005).
- [3] Heavy Flavor Averaging Group, www.slac.stanford.edu/xorg/hfag/charm/index.html (2010).
- [4] A. G. Akeroyd and C. H. Chen, Phys. Rev. D **75**, 075004 (2007).
- [5] B. A. Dobrescu and A. S. Kronfeld, Phys. Rev. Lett. **100**, 241802 (2008).
- [6] L. Widhalm *et al.* (Belle Collab.), Phys. Rev. Lett. **100**, 241801 (2008).
- [7] L. Widhalm *et al.* (Belle Collab.), Phys. Rev. Lett. **97**, 061804 (2006).
- [8] B. Aubert *et al.* (BaBar Collab.), Nucl. Instrum. Methods A **479**, 1 (2002).
- [9] W. Menges *et al.* (BaBar Collab.), IEEE Nuc. Sci. Symp. Conf. Rec. **5**, 1470 (2006).
- [10] D.J. Lange, Nucl. Instrum. Methods A **462**, 152 (2001).
- [11] T. Sjostrand, Computer Physics Commun. **82**, 74 (1994).
- [12] S. Agostinelli *et al.* (GEANT4 Collab.), Nucl. Instrum. Methods A **506**, 250 (2003).
- [13] E. Richter-Was, Phys. Lett. B **303**, 163 (1993).
- [14] C. Amsler *et al.* (Particle Data Group), Phys. Lett. B **667**, 1 (2008).
- [15] B. Aubert *et al.* (BaBar Collab.), Phys. Rev. Lett. **98**, 141801 (2007).
- [16] J.P. Lees *et al.* (BaBar Collab.), arXiv:1003.3063v2 (submitted to PRD-RC) (2010). Due to differences in the event reconstruction and analysis method we estimate this measurement to have a statistical error which is about 40% correlated with the present measurement and an uncorrelated systematic error.
- [17] L. Lyons, D. Gibut, P. Clifford, Nucl. Instrum. Methods A **270**, 110 (1988).
- [18] J. P. Alexander *et al.* (CLEO-c Collab.), Phys. Rev. Lett. **100**, 161804 (2008).
- [19] J. P. Alexander *et al.* (CLEO-c Collab.), Phys. Rev. D **79**, 052001 (2009); P. Naik *et al.* (CLEO-c Collab.), Phys. Rev. D **80**, 112004 (2009).